Research Paper

CO$_2$ balance of a secondary tropical peat swamp forest in Sarawak, Malaysia

Frankie Kiew[a,c,*], Ryuichi Hirata[d], Takashi Hirano[b], Guan Xhuan Wong[a,c], Edward Baran Aeries[c], Kevin Kemudang Musin[c], Joseph Wenceslaus Waili[c], Kim San Lo[c], Mariko Shimizu[e], Lulie Melling[c]

[a] Graduate School of Agriculture, Hokkaido University, Sapporo, 060-8589, Japan
[b] Research Faculty of Agriculture, Hokkaido University, Sapporo, 060-8589, Japan
[c] Sarawak Tropical Peat Research Institute, Lot 6035, Kuching-Kota Samarahan Expressway, 94300, Kota Samarahan, Malaysia
[d] National Institute for Environmental Studies, Tsukuba, 305-8506, Japan
[e] Civil Engineering Research Institute for Cold Region, Sapporo, 062-8602, Japan

A B S T R A C T

Tropical peat swamp forest (PSF) has accumulated a huge amount of carbon as peat over millennia, though the carbon rich ecosystem is now threatened with disturbances due to land-use change to industrial plantations of oil palm and pulp woods. Through the land conversion, peat carbon has become vulnerable and potentially changes to a great carbon dioxide (CO$_2$) source to the atmosphere. It is essential to quantify the CO$_2$ balance of the ecosystem and understand how the CO$_2$ balance responds to environmental changes to predict the role of PSF in global carbon cycles. However, filed studies based on the ecosystem-scale monitoring of CO$_2$ flux are quite limited. Thus, we began CO$_2$ flux monitoring over a secondary PSF in Sarawak, Malaysia, by the eddy covariance technique in 2010. Daily NEE and RE were significantly different between the dry and wet periods ($p < 0.01$), respectively, whereas no significant difference was found in daily GPP. As a result, the seasonal difference in NEE between the two periods ($0.52 \, \mathrm{g \, C \, m^{-2} \, d^{-1}}$) was due to that in RE ($0.57 \, \mathrm{g \, C \, m^{-2} \, d^{-1}}$). Daily RE was significantly greater in the dry period mainly because of lower groundwater level (GWL). Lower GWL enhances peat aeration and potentially increases oxidative peat decomposition, which results in higher soil CO$_2$ efflux. Annual NEE was $-136 \pm 51 \, \mathrm{g \, C \, m^{-2} \, yr^{-1}}$ (mean $\pm$ 1 standard deviation) during the four years until 2014. The negative annual NEE was equivalent to those of some tropical rain forests on mineral soil, but was more negative than $174 \, \mathrm{g \, C \, m^{-2} \, yr^{-1}}$ for an almost undrained PSF in Central Kalimantan, Indonesia (Hirano et al., 2012). The difference in annual NEE between the two sites is attributable to higher leaf area index and less distinct seasonality in precipitation in this site.

1. Introductions

Tropical peat carbon accounts for 11–14% of global peat carbon (Page et al., 2011). Southeast Asia's peatlands store approximately 65% (68.5 Gt) of total tropical peat carbon (104.7 Pg), including newly found peatland in Congo basin (Dargie et al., 2017). In southeast Asia, the largest distribution of peatlands is in Indonesia (84%, 21 Mha) followed by Malaysia (13%, 2–2.5 Mha) and the remains are found in Thailand, Vietnam, Brunei, and the Philippines (Murdiyarso et al., 2010; UNDP, 2006). Coexistence of tropical rainforest and waterlogged woody peat is the key characteristic that distinguishes the tropical peat ecosystem from temperate and boreal peatlands. High biomass productivity in conjunction with reduced carbon dioxide (CO$_2$) emission from soil under the anoxic condition induced by high groundwater level

(GWL) had made this ecosystem an efficient carbon (C) sink. However, this massive C stock now becomes vulnerable and consequently changed into a large C source to the atmosphere because of land conversion and peat fires (e.g. Hooijer et al., 2012; Miettinen et al., 2017; Jauhiainen et al., 2016a,b; Konecny et al., 2016; Page and Hooijer, 2016). In developing countries, land conversion is often driven by the needs for agriculture development for economic growth, and the consequential C emission is further aggrevated by the occurrence of peat fires caused by improper land preparation and El Niño events.

Local hydrology is reported as the main controlling factor of CO$_2$ emission from tropical peatlands, because fluctuation in both soil and air temperatures is much smaller than those of temperate and boreal peatlands. GWL lowering deepens the unsaturated peat layer and enhances peat aeration. As a result, oxidative peat decomposition

theoretically accelerates. Previous studies using the eddy covariance technique in tropical peat swamp forest (PSF) in Central Kalimantan (Hirano et al., 2007, 2009, 2012) showed GWL lowering caused a high ecosystem-scale CO_2 emission, associated with enhanced peat decomposition (Hirano et al., 2014). Sundari et al. (2012) also found a similar relationship of soil respiration with GWL using an automated chamber system. However, there is a report that CO_2 efflux through tropical peat decomposition showed a positive relationship with soil temperature despite a narrow temperature range (Jauhiainen et al., 2012). In addition, Melling et al. (2005) showed that the response of soil respiration in tropical peatlands to environmental factors depended on ecosystem types, including PSF, sago and oil palm plantations. Even in PSF, heterogeneity of underlying peat influences vegetation cover, because plants adapt to soil conditions. Peat depth, peat characteristics and nutrient availibity gradually change from the edge to the center of a peat dome, which is formed typically in ombrotrophic conditions. The peat distribution in peat domes has developed the zonal pattern of PSF, including mixed peat swamp, Alan Batu, Alan Bunga, Padang Alan, Padang Selusor and Padang Keruntum from the edge to the center. Toward the center, PSFs' structure changes to shorter and sparser (Anderson, 1964; Melling et al., 2007). In Central Kalimantan, Indonesia, Page et al. (1999) found similar distinct forest types (mixed peat swamp, low pole, tall interior and very low canopy forests) across the gradient of peat thickness and peat surface elevation. Hydrological conditions in relation to mineral and nutrient flows are more likely responsible for the formation of the different forest types rather than the direct influence of peat thickness and surface topography (Melling et al., 2007).

Reports on the ecosystem-scale CO_2 balance of tropical PSF using the eddy covariance technique were only so far from Central Kalimantan (Hirano et al., 2007, 2012). Thus, information based on field experiments is still limited. Given the fact that tropical PSF is heterogenous, and climate, especially the precipitation pattern, is highly variable in tropical regions, more field studies are necessary to cover the wide range of tropical PSF distribution, considering the variabilities of climate and peat characteristics. Therefore, we have measured CO_2 flux above a secondary PSF in Sarawak, Malaysia by the eddy covariance technique since 2011. Sarawak is located in the northwest coast of Borneo Island, facing South China Sea. In Sarawak, seasonal variation in precipitation is less distinct than in Central Kalimantan, and precipitation is less sensitive to ENSO events. In this study, using four-year-long data from 2011 to 2014, we investigated the environmental dependence of CO_2 fluxes, and the seasonal and interannual variations of CO_2 balance.

2. Materials and methods

2.1. Study site

The study site is a PSF located in Betong division of Sarawak, Malaysia. A 40-m-tall tower was constructed at around the center (1°23′59.42″N, 111°24′6.69″E) of a peat dome with an area of 25.6 km². The terrain is almost flat with the elevation of 17 m a.s.l. Peat depth around the tower is about 10 m. The forest was selectively logged and has regenerated as a secondary forest. Logging in the windward area (southeast direction from the tower) was almost terminated in 1980s, and the surrounding area of the forest was converted into oil palm plantations in 1990s. Originally, the tower site was at the border between Alan Bunga and Padang Alan forests. During succession, the forest has been dominated by *Litsea* spp., outgrew by some original trees of *Shorea albida*. Tree density was 1990 trees ha⁻¹ in 2016. In 2010 the canopy height was about 25 m. Plant area index (PAI) measured monthly from April 2013 to March 2014 with a plant canopy analyser (LAI2000, Li-Cor Inc., Lincoln, NE, USA) was 7.9 m² m⁻² on average; seasonal variation was not found in PAI. Microtopography consisting of hummocks and hollows exists on the forest floor, with considerable

amount of leaf litter accumulation. Saplings are also abundant below the canopy. The physical and chemical properties of peat soil were shown by Melling, (2013), in which this site was abbreviated as CA.

2.2. Flux and meteorological measurement

This paper presents data measured from 2011 to 2014. CO_2 and energy fluxes have been measured since October 2010 at the height of 41 m using the eddy covariance technique. A sonic anemometer/thermometer (CSAT3, Campbell Scientific Inc., Logan, UT, USA) and an open-path CO_2/H_2O analyzer (LI7500A, Li-Cor Inc.) were used to measure three-dimensional wind velocity, air temperature, CO_2 density and water vapor density at 10 Hz. CO_2 concentrations were also measured every minute at the heights of 41, 21, 11, 3, 1, and 0.5 m in a rotation using a closed-path CO_2 analyzer (LI-820, Li-Cor Inc.). Raw data were recorded with a data logger (CR3000, Campbell Scientific Inc.).

Global and reflected solar radiations and long-wave radiations (upward and downward) were measured using a radiometer (CNR4, Kipp & Zonen, Delft, the Netherlands) at the height of 41 m. Downward and upward photosynthetic photon flux densities (PPFD) were also measured at the same height using two quantum sensors (LI-190, Li-Cor Inc.). Wind speed and direction were measured with a vane and three-cup anemometer (Wind sentry, Young, Traverse City, MI, USA) at the height of 41m. Air temperature (T_a) and relative humidity (RH) were measured with a temperature & relative humidity probe (CS215, Campbell Scientific Inc.) in a radiation shield (41303-5A, Campbell Scientific Inc.) at the heights of 11 and 41 m, respectively. Water vapor pressure deficit (VPD) was calculated from T_a and RH. GWL was measured at one point with a water level logger (STS DN/L 50, Sensor Technik Sirnach AG, Danbury, CT, USA); GWL was the distance between the groundwater surface and the ground surface at a hollow. Volumetric soil water content (VWC) was measured in the uppermost 30-cm-thick layer at a hollow using a TDR sensor (CS615, Campbell Scientific Inc.). Soil temperature (T_s) was measured using resistance thermometers at 5 and 10 cm depths, respectively. Precipitation (PT) was measured using a tipping-bucket rain gauge (TE525, Campbell Scientific Inc.) at the height of 1 m in an open space close to the tower. These data were averaged and recorded half-hourly using a datalogger (CR3000, Campbell Scientific Inc.).

The measurement was occasionally interrupted mainly because of power problems. The resultant data gaps in PPFD, T_a and VPD were filled by linear regression with data measured on a tower (1°27′55″N, 111°09′20″E) in another PSF site, about 20 km away from this site. Missing PT was filled on a daily basis with data of a nearby meteorological station (Lingga) about 26 km away; root mean square errors (RMSEs) were 11 mm d⁻¹ and 51 mm month⁻¹, respectively, on daily and monthly bases. Missing GWL was estimated hydrologically by the tank model method (Sugawara, 1979).

2.3. Flux calculation

Half-hourly mean CO_2 flux (F_C) was calculated from raw eddy data using a software, Flux Calculator (Ueyama et al., 2012). Through the calculation, spike removal (Vickers and Mahrt, 1997), planar fit rotation (Wilczak et al., 2001), frequency response correction (Massman, 2000) and air density fluctuation correction (Webb et al., 1980) were applied. CO_2 storage below the flux measurement height was estimated at intervals of 5 min from CO_2 concentrations measured at the six heights (Section 2.2) by temporal linear interpolation (Hirano et al., 2007). Then, we calculated half-hourly CO_2 storage flux (F_S) as the change of CO_2 storage. Finally, the net ecosystem exchange (NEE) of CO_2 was calculated as the sum of F_C and F_S (NEE = F_C + F_S). Positive NEE indicates that the ecosystem is a net CO_2 source, whereas negative NEE indicating a net CO_2 sink.

2.4. Quality control, gap filling and partitioning of NEE

Prior to gap-filling, NEE data were screened by the mean absolute deviation (MAD) spike detection method (Papale et al., 2006) and the deviation of each half-hourly NEE from mean diurnal variation (MDV). MDV and standard deviation (SD) were calculated for a 14-day-long moving window. If NEE was out of 3 SDs $\pm$ MDV, it was removed. NEE under low turbulent conditions during the nighttime (PPFD $\leq$ 10 µmol m^{-2} s^{-1}) was filtered using a friction velocity (u*) threshold determined using Flux Analysis Tool software (Ueyama et al., 2012); the u* threshold was determined at 0.15 m s^{-1} at this site. Finally, the gaps were filled using the marginal distribution sampling (MDS) method (Reichstein et al., 2005). The size of moving windows was between 7 and 49 days depending on the length of data gaps and the availability of "look up" values. We performed gap filling separately for the daytime (PPFD $>$ 10 µmol m^{-2} s^{-1}) and the nighttime (PPFD $\leq$ 10 µmol m^{-2} s^{-1}). Following a flux study in PSFs (Hirano et al., 2012), PPFD, VPD and T_a were used during the daytime, whereas GWL, T_s and VWC were used during the nighttime. Missing NEE was "looked up" based on similar environmental conditions of $\pm$ 25 µ mol m^{-2} s^{-1} for PPFD, 0.15 kPa for VPD, 2.5 cm for GWL, 0.05 m^3 m^{-3} for VWC, 1.0 °C for T_a and 0.2 °C for T_s. Daytime ecosystem respiration (RE) was "looked up" from nighttime NEE using the same algorithm for gap-filling (MDS). Then, gross primary production (GPP) was calculated as the difference between NEE and RE (NEE = RE − GPP). During the nighttime, GPP was set to zero.

2.5. Light response parameters of NEE

Ecosystem photosynthetic parameters were calculated by fitting a non-rectangular hyperbola function (Eq. (1)) to measured PPFD and daytime NEE.

$$\text{NEE} = -\frac{1}{2\theta}(\alpha PPFD + P_{max} - \sqrt{(\alpha PPFD + P_{max} - 4\alpha P_{max}\theta PPFD)} + RE_d \tag{1}$$

where θ is the curvature (set to be 0.9), α is the initial slope, P_{max} is the maximum GPP, and RE_d is the dark respiration. Fitting was conducted on a daily basi. The photosynthetic parameter P_{max} was assessed for seasonality together with GPP.

2.6. Definition of the wet and dry periods

The driest month with the least PT generally occurs in June or July in this area (Fig. 1a). In the tropics, a threshold of monthly PT $<$ 100 mm is commonly used to determine the dry season (e.g. Malhi et al., 2002). According to this threshold, the dry season was very short in this site, because monthly PT barely droped below 100 mm. Thus, to extract a relatively dry period, we analyzed monthly PT using 15-year-long data at Lingga meteorological station (as mentioned above). As a result, the median of monthly PT (238 mm) was used to separate the relatively dry period and the wet period. The durations of each period are shown in Table 1. Conventionally, a hydrological year was determined to be from the onset of a dry period to the end of the next wet period. According to the PT threshold, the onset of the dry period shifted year by year (Table 1). The hydrological years were named Y1, Y2, Y3 and Y4, respectively, during the duration from April 2011 to September 2014 (Fig. 1a and Table 1).

2.7. Statistical analysis

The means of NEE, RE, GPP and environmental factors were compared between the dry and wet periods by t-test. Those of each period were compared by Tukey's HSD. Regression coefficients of light-saturated NEE with VPD were compared between the two periods by t-test. These analyses were performed using R version 3.3.1 software.

3. Results

3.1. Seasonal and interannual variations of environmental factors

Seasonality in PT was partly attributable to ENSO events; a La Niña event occurred from 2010 to early 2012, and weak El Niño events occurred in 2012 and 2014, which are determined by sea surface temperature (SST) anomalies (http://www.cpc.ncep.noaa.gov/). The longest wet period was in Y1 (8 months) in relation to a La Niña event, and the dry period was longest in Y3 (8 months) (Table 1). The driest month (monthly PT $<$ 100 mm) was generally recorded in June or July, whereas it occurred also in Februay in 2014 (Fig. 1a). Cumulative PT in the dry periods accounted for 22.1, 43.5, 43.7 and 61.2% of total PT in Y1, Y2, Y3 and Y4, respectively, whereas mean montly PT was significantly lower in the dry period (Table 2). Annual PTs on a calender basis in 2011, 2012, 2013 and 2014 were 2965, 2729, 2563 and 2120 mm, respectively (Table 3). Following the seasonality of PT, GWL decreased in the dry period (Fig. 1b). On average, GWL was −9 cm in the wet period and −29 cm in the dry period (Table 2). During the wet period in 2011 (W1), GWL rose up to 30 cm aboveground, but only for a short period. In this site, however, flooding was uncommon even during the wet period. The lowest GWL of −67 cm was recorded in the 2011 dry period (D1). Correspondingly, VWC was significantly lower during the dry period ($p < 0.01$, Table 2).

Daily PPFD was significantly lower by 6% during the wet period ($p < 0.01$, Table 2) following the increase in PT (Fig. 1a and Table 2). The lowest daily PPFD was recorded in the W2 (32.6 mol m^{-2} d^{-1}), and the highest was in the D1 and D2 (35.8 mol m^{-2} d^{-1}, Table 2). Annual PPFD in 2011, 2012, and 2014 was the same at 12.5 kmol m^{-2} yr^{-1}, but increased slightly to 12.8 kmol m^{-2} yr^{-1} in 2013 (Table 3). Daily mean T_a at the height of 41 m fluctuated between 23 and 30 °C (Fig. 1d). Daily minimum and maximum T_a ranged from 19.8 to 25.9 °C and from 24.5 to 35.5 °C, respectively (data not shown). Mean T_a was significantly higher in the dry period ($p < 0.01$), but the difference was small (0.7 °C, Table 2). Both daily minimum and maximum T_a increased in the dry period similarly to daily mean T_a. Annual mean T_a was almost constant between 26.4 and 26.6 °C. Daily mean T_s increased linearly with daily mean T_a (data not shown). Daytime VPD was also significantly higher in the dry period (Table 2), probably owing to increased T_a. The lowest VPD was generally recorded in early-January and gradually increased to its peak in late June (Fig. 1e). Daytime VPDs during D1 and D2 were significantly higher than those in the other dry periods (Table 2).

3.2. Environmental control on CO_2 flux

In order to investigate the response of RE to environmental conditions, measured NEE (RE) was plotted against GWL and VWC. Nighttime NEE increased significantly as GWL ($r = -0.53$, $p = 0.01$) or VWC ($r = -0.42$, $p = 0.04$) lowered (Fig. 2). According to the relationship, RE increased linearly by 0.28 µmol m^{-2} s^{-1} for every 10 cm lowering in GWL, and RE was 8.5 µmol m^{-2} s^{-1} when GWL was 0 cm.

Photosynthetic response was analyzed using light-saturated NEE (PPFD $>$ 1000 µmol m^{-2} s^{-1}) instead of GPP to avoid uncertainties caused by flux partitioning procedures. Fig. 3 shows the response of light-saturated NEE to VPD in the dry and wet periods. Light-saturated NEE showed a positive relationship with VPD ($p < 0.01$) in both periods; there was no significant difference in the regression coeficients between the two periods ($p > 0.05$). Means ($\pm$ 1 SD) of light-saturated NEE in the dry and wet periods were −18.2 $\pm$ 9.0 and −19.1 $\pm$ 9.0 µmol m^{-2} s^{-1}, respectively. Maximum GPP (P_{max}) was 33.7 and 34.1 µmol m^{-2} s^{-1}, respectively, on average in the dry and wet periods (Table 2); these were not significantly different.
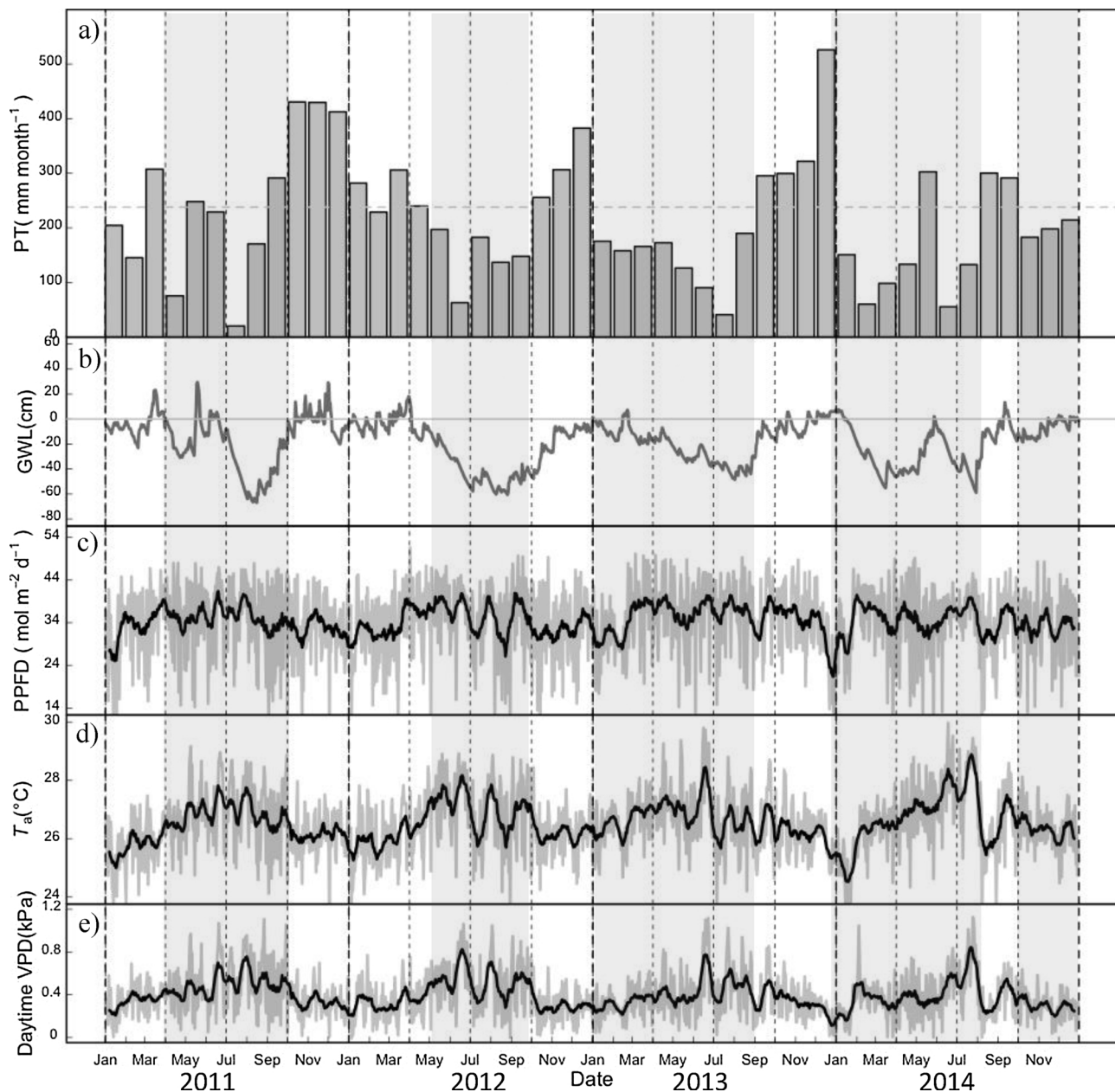
Fig. 1. Seasonal variations of monthly precipitation (PT) (a), daily mean groundwater level (GWL) (b), daily photosynthetic photon flux density (PPFD) (c), daily mean air temperature (T_a) (d) and daytime mean vapor pressure deficit (VPD) (e) from January 2011 to December 2014. Black lines are 14-day-long moving averages. Bold dashed vertical lines are the border of calendar years. The horizontal dotted line in (a) is the median of 15-year-long PT data measured at Lingga station. Grey areas denote the dry periods.

3.3. Seasonality of CO_2 fluxes

Seasonal variations in daily NEE, RE and GPP are shown in Fig. 4. In general, daily NEE was more positive in the dry periods and became slightly neutral or more negative in the wet periods (Table 2). Daily RE varied similarly with NEE. The variation of daily GPP was smaller than RE. Daily NEE and RE were significantly different between the two periods ($p < 0.01$), respectively, whereas no significant difference was found in daily GPP ($p > 0.05$) (Table 2). As a result, the seasonal difference in NEE ($0.52\,\mathrm{g\,C\,m^{-2}\,d^{-1}}$) was due to RE ($0.57\,\mathrm{g\,C\,m^{-2}\,d^{-1}}$).

3.4. Annual CO_2 fluxes

Annual NEE was negative and ranged from -207 (2011) to $-98\,\mathrm{g\,C\,m^{-2}\,yr^{-1}}$ (2012) in four years with a mean $\pm$ 1 SD of

$-136 \pm 51\,\mathrm{g\,C\,m^{-2}\,yr^{-1}}$, resulting from GPP of $3682 \pm 149\,\mathrm{g\,C\,m^{-2}\,yr^{-1}}$ and RE of $3546 \pm 149\,\mathrm{g\,C\,m^{-2}\,yr^{-1}}$ (Table 3). On the other hand, both annual RE and GPP showed their highest and lowest values in 2013 and 2014, respectively (Table 3). The rank orders of NEE and RE or GPP were inconsistent. NEE showed a negative relationship with GWL ($r = -0.92$, data not shown), though it was not significant ($p = 0.08$) because of a small sample size ($n = 4$). RE and GPP had no relationship with GWL ($r = -0.14$ and 0.17, respectively). In addition, relationship with PT or PPFD was weak ($r^2 < 0.49$) for NEE, RE and GPP.

4. Discussion

Seasonal variation in PT was not so clear in this study site during the four years. Only one or two dry months defined as monthly PT less than 100 mm appeared per calendar year (Fig. 1a). Thus, the relatively dry

Table 1
Duration of the wet and dry periods from 2011 to 2014. Duration between the onset of a dry period and the end of the subsequent wet period was defined as one hydrological year named as Y1, Y2, Y3 and Y4, respectively.

Year		Period	Duration			Length (Months)
2011–2012	(Y1)	Dry (D1)	April 2011	–	August 2011	5
		Wet (W1)	September 2011	–	April 2012	8
2012–2012	(Y2)	Dry (D2)	May 2012	–	September 2012	5
		Wet (W2)	October 2012	–	December 2012	3
2013–2013	(Y3)	Dry (D3)	January 2013	–	August 2013	8
		Wet (W3)	September 2013	–	December 2013	4
2014–2014	(Y4)	Dry (D4)	January 2014	–	July 2014	7
		Wet (W4)	August 2014	–	September 2014	2

period and the wet period were differentiated using median (238 mm) of monthly PT from 15-year-long data recorded at a nearby meteorological station. As a result, daily NEE was significantly less negative in the dry period than in the wet period (Table 2). The seasonal difference of NEE between the dry and wet periods was 0.53 g C m^{-2} d^{-1} on average, which was almost equivalent to that of RE (0.57 g C m^{-2} d^{-1}). Daily RE was significantly greater in the dry period mainly because of lower GWL or VWC (Fig. 2). Lower GWL enhances peat aeration and potentially increases oxidative peat decomposition, which results in higher soil CO_2 efflux (e.g. Hirano et al., 2012 2014). In contrast, daily GPP showed no siginificant seasonal differences (Table 2) probably because of compensation effects between PPFD and VPD. In the wet period, although lower PPFD decreased GPP, lower daytime VPD eased the reduction in light-saturated NEE due to stomatal closure (Fig. 3). Also, maximum GPP (P_{max}) showed no significant seasonal difference (Table 2). Moreover, plant area index (PAI) showed no seasonal variation. These results suggest that the fluctuation in GWL between 0 and −60 cm did not influence the photosynthetic parameters of this ecosystem. A study in Amazonian rainforest by Goulden et al. (2004) found a reduction in photosynthesis which started right before the onset of the dry period, owing to the adaptation by the vegetation to avoid severe drought stress. Although it is unclear how the ecosystem's photosynthesis might respond to the drier environment in the future, lack of such adaptation might cause disruption in the photosynthetic component of the CO_2 exchange, thus could alter the ecosystem's CO_2 dynamic.

The secondary peat swamp forest had functioned as a net CO_2 sink of 136 ± 51 g C m^{-2} yr^{-1} during the four years (Table 3). In comparison with flux studies using the eddy covariance technique in tropical humid forest, the negative annual NEE was equivalent to those of tropical rain forests on mineral soil in Peninsula Malaysia (−124 g C m^{-2} yr^{-1}, Kosugi et al., 2008) and in French Guiana (−138 g C m^{-2} yr^{-1}, Bonal et al., 2008), whereas it was less negative than the mean of 29 tropical humid evergreen forests (−403 ± 102 g C m^{-2} yr^{-1} (originaly in NEP), Luyssaert et al., 2007). In constract, the annual NEE (−136 g C m^{-2} yr^{-1}) was more negative than that of an almost undrained PSF in Central Kalimantan, Indonesia (Hirano et al., 2012); mean annual NEE was 174 ± 203 g C m^{-2} yr^{-1} for four years including an El Niño event. The large NEE difference of 310 g C m^{-2} yr^{-1} on average between the two sites (Hirano et al. − this study) resulted from both GPP (−214 g C m^{-2} yr^{-1}) and RE (96 g C m^{-2} yr^{-1}) differences. The higher GPP in this study was attributable to higher PAI; 7.9 m^2 m^{-2} (this study) vs. 5.0 m^2 m^{-2} (Hirano et al., 2012). The lower RE in this study was probably due to higher minimum GWL despite similar mean

Table 2
Means of daily CO_2 fluxes and environmental variables in each period (mean ± 1 standard deviation (SD)).

Period	NEE (g C m^{-2} d^{-1})		RE (g C m^{-2} d^{-1})		GPP (g C m^{-2} d^{-1})		P_{max} (µmol m^{-2} s^{-1})		PPFD (mol m^{-2} d^{-1})		Daytime VPD (kPa)		T_a (°C)		VWC (m^3 m^{-3})		GWL (cm)		PT (mm month^{-1})	
D1	−0.76 ±	2.04bc	9.09 ±	2.75b	9.85 ±	1.84bc	33.2 ±	9.7ab	35.8 ±	8.0a	0.77 ±	0.31a	26.9 ±	1.0a	–		−27.6 ±	22.9de	149 ±	98
D2	0.40 ±	2.06a	10.85 ±	3.38a	10.45 ±	2.74ab	35.6 ±	9.7ab	35.8 ±	8.4a	0.81 ±	0.34a	27.0 ±	1.2a	0.50 ±	0.14e	−41.5 ±	13.7f	146 ±	52
D3	−0.23 ±	2.09abc	10.53 ±	1.94a	10.76 ±	1.52a	33.5 ±	9.8ab	35.7 ±	8.0a	0.67 ±	0.30b	26.8 ±	1.0ab	0.69 ±	0.15c	−23.0 ±	13.5 cd	140 ±	51
D4	−0.14 ±	2.24ab	9.10 ±	2.13b	9.24 ±	1.96c	32.8 ±	10.6a	35.1 ±	7.9ab	0.63 ±	0.28bc	26.8 ±	1.3ab	0.62 ±	0.18d	−28.6 ±	16.8e	133 ±	83
W1	−0.92 ±	2.05c	9.39 ±	2.14b	10.30 ±	1.68ab	33.3 ±	9.3ab	33.2 ±	8.5b	0.62 ±	0.29bcd	26.2 ±	1.0c	–		−6.3 ±	14.0a	328 ±	84
W2	−0.49 ±	2.26bc	8.81 ±	2.78b	9.30 ±	1.86c	31.8 ±	8.7b	32.6 ±	8.2b	0.52 ±	0.24d	26.2 ±	0.7c	0.74 ±	0.13bc	−17.5 ±	12.5bc	315 ±	64
W3	−0.70 ±	2.19bc	9.42 ±	1.80b	10.12 ±	1.75ab	37.1 ±	11.1a	33.9 ±	8.1ab	0.57 ±	0.26cd	26.2 ±	0.9c	0.83 ±	0.07a	−5.3 ±	8.0a	361 ±	111
W4	−0.21 ±	1.84abc	9.81 ±	2.11ab	10.02 ±	2.12abc	34.6 ±	12.4ab	33.2 ±	8.0b	0.53 ±	0.24cd	26.4 ±	1.2bc	0.81 ±	0.11ab	−11.1 ±	11.3ab	296 ±	6
Dry	−0.18		9.91		10.09		33.7		35.5		0.71		26.9		0.62		−29.2		141	
Wet	−0.71		9.34		10.05		34.1		33.3		0.58		26.2		0.82		−8.6		329	
Sig. (t-test)	***		***		NS		NS		***		***		***		***		***		***	

Values marked with the different letter in each column are significantly different ($p < 0.05$) according to Tukey's HSD test. As for seasonal means, t-test was applied (***: $p < 0.01$). NS indicates no significant different between seasons.

Table 3
Annual CO_2 balance and annual mean environmental variables from 2011 to 2014 on a calendar basis.

Year	NEE (g C m^{-2})	RE	GPP	PPFD (kmol m^{-2})	GWL (cm)	PT (mm)
2011	−207	3450	3657	12.5	−15.7	2965
2012	−98	3633	3731	12.5	−22.8	2729
2013	−140	3708	3848	12.8	−17.1	2563
2014	−100	3392	3492	12.5	−20.3	2120
Mean ± SD	−136 ± 51	3546 ± 149	3682 ± 149	12.6 ± 0.2	−19.0 ± 3.2	2594 ± 356

annual GWL (−19 cm vs. −14 cm); GWL lowered to −1 m on a monthly basis in 2006, an El Niño year, even at the almost undrained PSF in Central Kalimantan. The annual NEE showed a negative linear relationship with annual mean GWL ($r^2 = 0.92$), though it was not significant ($p = 0.08$) because of a small sample size ($n = 4$). If the significance level of $p < 0.10$ is allowed, the linearity suggests that every lowering of GWL by 10 cm increases NEE by 133 g C m^{-2} yr^{-1}. Such linearity between annual NEE and annual mean GWL was also found in PSFs in Central Kalimantan with the slopes of 238 and 161 g C m^{-2} yr^{-1} against 10-cm GWL lowering, respectively, in the almost undrained and drained PSFs (Hirano et al., 2012). In this site, the sensitivity of NEE to GWL was probably lower than those in Central Kalimantan (CK). The difference might be related to differences in peat depth (10 m (this study) vs. 3–4 m (CK)) and peat formation history (costal peat (this study) vs. inland peat (CK), Dommain et al., 2011).

To assess C balance, not only eddy CO_2 flux but also C leaching through water discharge should be considered. Moore et al. (2013) reported that 62.5 and 105.3 g C m^{-2} yr^{-1} were lost as organic carbon (dissolved organic carbon (DOC) + particulate organic carbon (POC)), respectively, from an intact peat swamp forest and a moderately disturbed peat swamp forest in Central Kalimantan. Moreover, about 10 g C m^{-2} yr^{-1} of annual methane emissions was assessed in a nearby undrained tropical peat swamp forest in Sarawak (Wong et al., submitted). Thus, if these C losses are considered, the secondary peat swamp forest could be a slight C sink or a C neutral.

5. Conclusions

Our study showed the CO_2 balance of a secondary peat swamp forest developed in a humid climate with a relatively short dry period. Seasonal variation in NEE was mainly governed by RE which was negatively related to GWL. The CO_2 balance of the peat swamp forest was sensitive to GWL similar to the previous studies. In the warming climate, there is a prediction that El Niño drought will be intensified in the western area of the equatorial Pacific Ocean (Power et al., 2013). Moreover, Cai et al. (2014) predicts that extremely strong positive Indian Ocean Dipole (IOD) modes will increase, and consequently the frequency of drought will also increase in the eastern area of Indian Ocean. Although the peat swamp forest was a net CO_2 sink but almost C
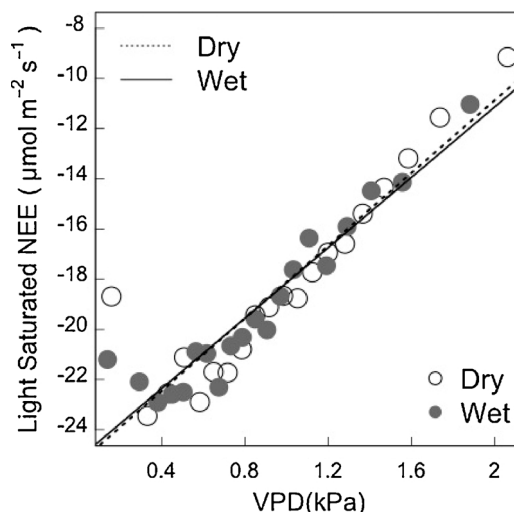
Fig. 3. Response of NEE to vapor pressure deficit (VPD) in light-saturated conditions (PPFD > 1000 μmol m^{-2} s^{-1}). Half-hourly measured NEE was plotted against VPD separately for the dry and wet periods. NEE data were sorted according to VPD and binned into 20 classes in the same size. Lines were drawn for significant relationship ($p < 0.01$).

neutral during the four years from 2011 to 2014, it potentially shifts to a C source in the future under the drier environment.
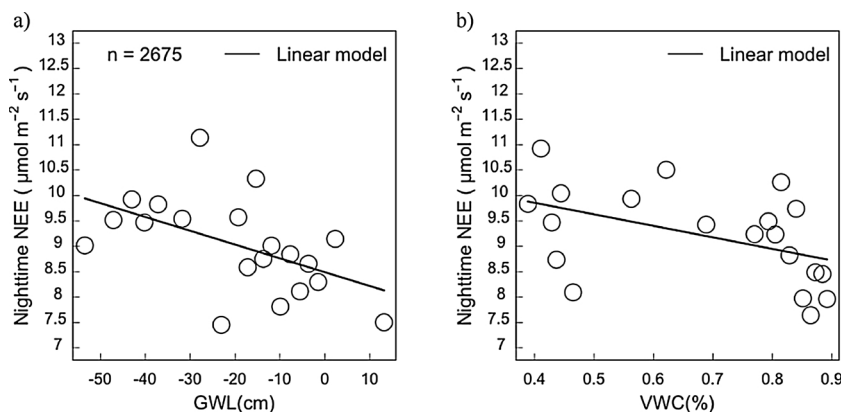
Fig. 2. Relationship between measured nighttime NEE and groundwater level (GWL) (a) or soil water content (VWC) (b). Half-hourly NEE data were sorted according to GWL or VWC and bin-averaged for 20 classes in the same size. Lines were drawn for significant relationship (p < 0.05).
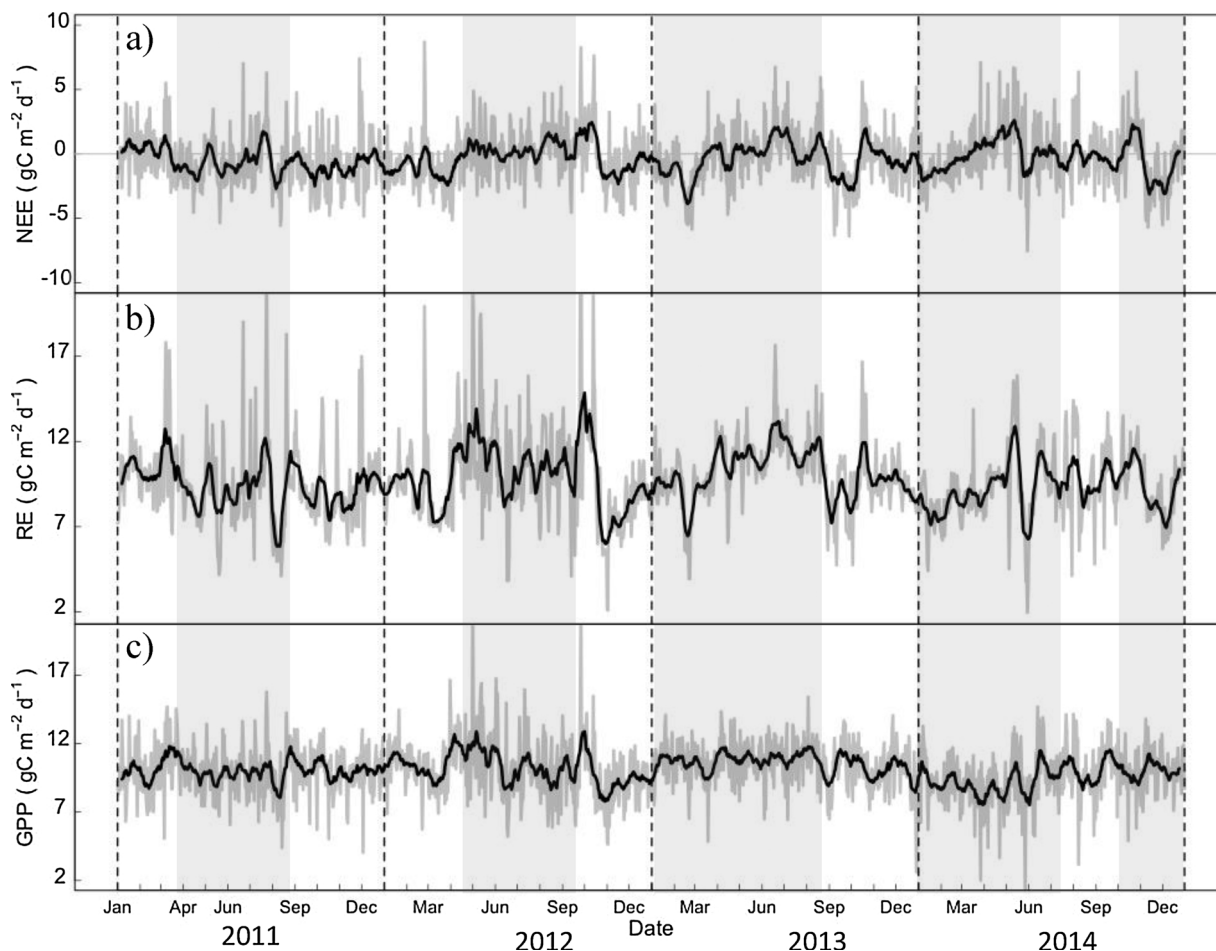
Fig. 4. Seasonal variation in daily values of NEE (a), RE (b) and GPP (c) from January 2011 to December 2014 (grey lines) after gap-filling. Black lines are 14-day-long moving averages. Grey shades indicate the dry periods. Dotted vertical lines are the calendar year border.

References

Anderson, J.A.R., 1964. The structure and development of the peat swamps of Sarawak and Brunei. J. Trop. Geogr. 18, 7–16.

Bonal, D., Bosc, A., Ponton, S., Goret, J.-Y., Burban, B., Gross, P., Bonnefond, J.-M., Elbers, J., Longdoz, B., Epron, D., Guehl, J.-M., Granier, A., 2008. Impact of severe dry season on net ecosystem exchange in the Neotropical rainforest of French Guiana. Glob. Chang. Biol. 14, 1917–1933. http://dx.doi.org/10.1111/j.1365-2486.2008. 01610.x.

Cai, W., Santoso, A., Wang, G., Weller, E., Wu, L., Ashok, K., Masumoto, Y., Yamagata, T., 2014. Increased frequency of extreme Indian Ocean Dipole events due to greenhouse warming. Nature 510, 254–258. http://dx.doi.org/10.1038/nature13327.

Dargie, G.C., Lewis, S.L., Lawson, I.T., Mitchard, E.T.A., Page, S.E., Bocko, Y.E., Ifo, S.A., 2017. Age, extent and carbon storage of the central Congo Basin peatland complex. Nature 542, 86–90. http://dx.doi.org/10.1038/nature21048.

Dommain, R., Couwenberg, J., Joosten, H., 2011. Development and carbon sequestration of tropical peat domes in south-east Asia: links to post-glacial sea-level changes and Holocene climate variability. Quat. Sci. Rev. 30, 999–1010.

Goulden, M.L., Miller, S.D., Da Rocha, H.R., Menton, M.C., De Freitas, H.C., Silva Figueira, E.A.M., Dias De Sousa, C.A., 2004. Diel and seasonal patterns of tropical forest CO₂ exchange. Ecol. Appl. 14, 42–54. http://dx.doi.org/10.1890/02-6008.

Hirano, T., Segah, H., Harada, T., Limin, S., June, T., Hirata, R., Osaki, M., 2007. Carbon dioxide balance of a tropical peat swamp forest in Kalimantan, Indonesia. Glob. Chang. Biol. 13, 412–425. http://dx.doi.org/10.1111/j. 1365-2486.2006.01301.x.

Hirano, T., Jauhiainen, J., Inoue, T., Takahashi, H., 2009. Controls on the carbon balance of tropical peatlands. Ecosystems 12, 873–887. http://dx.doi.org/10.1007/s10021-008-9209-1.

Hirano, T., Segah, H., Kusin, K., Limin, S., Osaki, M., 2012. Effects of disturbances on the carbon balance of tropical peat swamp forests. Glob. Chang. Biol. 18, 3410–3422.

Hirano, T., Kusin, K., Limin, S., Osaki, M., 2014. Carbon dioxide emissions through oxidative peat decomposition on a burnt tropical peatland. Glob. Chang. Biol. 20, 555–565. http://dx.doi.org/10.1111/gcb.12296.

Hooijer, A., Page, S., Jauhiainen, J., Lee, W.A., Lu, X.X., Idris, A., Anshari, G., 2012. Subsidence and carbon loss in drained tropical peatlands. Biogeosciences 9, 1053–1071. http://dx.doi.org/10.5194/bg-9-1053-2012.

Jauhiainen, J., Hooijer, A., Page, S., 2012. Carbon dioxide emissions from an Acasia plantation on peatland in Sumatra, Indonesia. Biogeosciences 9, 617–630.

Jauhiainen, J., Page, S.E., Vasander, H., 2016a. Greenhouse gas dynamics in degraded and restored tropical peatlands. Mires Peat 17, 1–12. http://dx.doi.org/10.19189/MaP.2016.OMB.229.

Jauhiainen, J., Silvennoinen, H., Könönen, M., Limin, S., Vasander, H., 2016b. Management driven changes in carbon mineralization dynamics of tropical peat. Biogeochemistry 129, 115–132. http://dx.doi.org/10.1007/s10533-016-0222-8.

Konecny, K., Ballhorn, U., Navratil, P., Jubanski, J., Page, S.E., Tansey, K., Hooijer, A., Vernimmen, R., Siegert, F., 2016. Variable carbon losses from recurrent fires in drained tropical peatlands. Global Change Biol. 22, 1469–1480. http://dx.doi.org/10.1111/gcb.13186.

Kosugi, Y., Takanashi, S., Ohkubo, S., Matsuo, N., Tani, M., Mitani, T., Tsutsumi, D., Nik, A.R., 2008. CO₂ exchange of a tropical rainforest at Pasoh in Peninsular Malaysia. Agric. For. Meteorol. 148, 439–452. http://dx.doi.org/10.1016/j.agrformet.2007.10.007.

Luyssaert, S., Inglima, I., Jung, M., Richardson, A.D., Reichstein, M., Papale, D., Piao, S.L., Schulze, E.D., Wingate, L., Matteucci, G., Aragao, L., Aubinet, M., Beer, C., Bernhofer, C., Black, K.G., Bonal, D., Bonnefond, J.M., Chambers, J., Ciais, P., Cook, B., Davis, K.J., Dolman, A.J., Gielen, B., Goulden, M., Grace, J., Granier, A., Grelle, A., Griffis, T., Grünwald, T., Guidolotti, G., Hanson, P.J., Harding, R., Hollinger, D.Y., Hutyra, L.R., Kolari, P., Kruijt, B., Kutsch, W., Lagergren, F., Laurila, T., Law, B.E., Le Maire, G., Lindroth, A., Loustau, D., Malhi, Y., Mateus, J., Migliavacca, M., Misson, L., Montagnani, L., Moncrieff, J., Moors, E., Munger, J.W., Nikinmaa, E., Ollinger, S.V., Pita, G., Rebmann, C., Roupsard, O., Saigusa, N., Sanz, M.J., Seufert, G., Sierra, C., Smith, M.L., Tang, J., Valentini, R., Vesala, T., Janssens, I.A., 2007. CO₂ balance of boreal, temperate, and tropical forests derived from a global database. Glob. Chang. Biol. 13, 2509–2537. http://dx.doi.org/10.1111/j.1365-2486.2007.01439.x.

Malhi, Y., Pegoraro, E., Nobre, A.D., Pereira, M.G.P., Grace, J., Culf, A.D., Clement, R., 2002. Energy and water dynamics of a central Amazonian rain forest. J. Geophys. Res. Atmos. 107, 8061. http://dx.doi.org/10.1029/2001JD000623.

Massman, W.J., 2000. A simple method for estimating frequency response corrections for eddy covariance systems. Agric. For. Meteorol. 104, 185–198. http://dx.doi.org/10.1016/S0168-1923(00)00164-7.

Melling, L., Hatano, R., Goh, K.J., 2005. Soil CO₂ flux from three ecosystems in tropical peatland of Sarawak, Malaysia. Tellus, Ser. B Chem. Phys. Meteorol. 57, 1–11. http://dx.doi.org/10.1111/j.1600-0889.2005.00129.x.

Melling, L., Goh, K.J., Uyo, L.J., Sayok, A., Hatano, R., 2007. Biophysical characteristics

of tropical peatland. Proc. Soil Sci. Conf. Malaysia 1917, 17–19.

Melling, L., 2013. Greenhouse gas (GHG) emission from tropical peatland. Planter 89, 725–730.

Miettinen, J., Shi, C., Liew, S.C., 2017. Fire distribution in peninsular Malaysia, Sumatra and Borneo in 2015 with special emphasis on peatland fires. Environ. Manage. 1–11. http://dx.doi.org/10.1007/s00267-017-0911-7.

Moore, S., Evans, C.D., Page, S.E., Garnett, M.H., Jones, T.G., Freeman, C., Hooijer, A., Wiltshire, A.J., Limin, S.H., Gauci, V., 2013. Deep instability of deforested tropical peatlands revealed by fluvial organic carbon fluxes. Nature 493, 660–663. http://dx.doi.org/10.1038/nature11818.

Murdiyarso, D., Hergoualc'h, K., Verchot, L.V., 2010. Opportunities for reducing greenhouse gas emissions in tropical peatlands. Proc. Natl. Acad. Sci. U. S. A. 19655–19660. http://dx.doi.org/10.1073/pnas.0911966107.

Page, S.E., Hooijer, A., 2016. In the line of fire: the peatlands of Southeast Asia. Philos. Trans. R. Soc. B Biol. Sci. 371, 20150176. http://dx.doi.org/10.1098/rstb.2015.0176.

Page, S.E., Rieley, J.O., Shotyk, W., Weiss, D., 1999. Interdependence of peat and vegetation in a tropical peat swamp forest. Philos. Trans. R. Soc. Lond. B. Biol. Sci. 354, 1885–1897. http://dx.doi.org/10.1098/rstb.1999.0529.

Page, S.E., Rieley, J.O., Banks, C.J., 2011. Global and regional importance of the tropical peatland carbon pool. Glob. Chang. Biol. 17, 798–818. http://dx.doi.org/10.1111/j.1365-2486.2010.02279.x.

Papale, D., Reichstein, M., Aubinet, M., Canfora, E., Bernhofer, C., Kutsch, W., Longdoz, B., Rambal, S., Valentini, R., Vesala, T., Yakir, D., 2006. Towards a standardized processing of net ecosystem exchange measured with eddy covariance technique: algorithms and uncertainty estimation. Biogeosciences 3, 571–583. http://dx.doi.org/10.5194/bg-3-571-2006.

Power, S., Delage, F., Chung, C., Kociuba, G., Keay, K., 2013. Robust twenty-first-century projections of El Niño and related precipitation variability. Nature 502, 541–545.

http://dx.doi.org/10.1038/nature12580.

Reichstein, M., Falge, E., Baldocchi, D., Papale, D., Aubinet, M., Berbigier, P., Bernhofer, C., Buchmann, N., Gilmanov, T., Granier, A., Grünwald, T., Hávranková, K., Ilvesniemi, H., Janous, D., Knohl, A., Laurila, T., Lohila, A., Loustau, D., Matteucci, G., Meyers, T., Miglietta, F., Ourcival, J.M., Pumpanen, J., Rambal, S., Rotenberg, E., Sanz, M., Tenhunen, J., Seufert, G., Vaccari, F., Vesala, T., Yakir, D., Valentini, R., 2005. On the separation of net ecosystem exchange into assimilation and ecosystem respiration: review and improved algorithm. Glob. Chang. Biol. 11, 1424–1439. http://dx.doi.org/10.1111/j.1365-2486.2005.001002.x.

Sugawara, M., 1979. Automatic calibration of the tank model/L'étalonnage automatique d'un modèle à cisterne. Hydrol. Sci. Bull. 24, 375–388. http://dx.doi.org/10.1080/02626667909491876.

Sundari, S., Hirano, T., Yamada, H., Kusin, K., Limin, S., 2012. Effect of groundwater level on soil respiration in tropical peat swamp forests. J. Agric. Meteorol. 68, 121–134. http://dx.doi.org/10.2480/agrmet.68.2.6.

UNDP, 2006. Malaysia's peat swamp forets: conservation and sustainable use, united nations development programme (UNDP), Malaysia. http://dx.doi.org/10.1017/CBO9781107415324.004.

Ueyama, M., Hirata, R., Mano, M., Hamotani, K., Harazono, Y., Hirano, T., Miyata, A., Takagi, K., Takahashi, Y., 2012. Influences of various calculation options on heat, water and carbon fluxes determined by open- and closed-path eddy covariance methods. Tellus B 64. http://dx.doi.org/10.3402/tellusb.v64i0.19048.

Vickers, D., Mahrt, L., 1997. Quality control and flux sampling problems for tower and aircraft data. J. Atmos. Oceanic Technol. 14, 512–526. http://dx.doi.org/10.1175/1520-0426(1997)014<0512:QCAFSP>2.0.CO;2.

Webb, E.K., Pearman, G.I., Leuning, R., 1980. Correction of flux measurements for density effects due to heat andwater vapour transfer. Q. J. R. Meteorol. Soc. 106, 85–100.

Wilczak, J., Oncley, S., Stage, S., 2001. Sonic anemometer tilt correction algorithms. Boundary-Layer Meteorol. 99, 127–150.